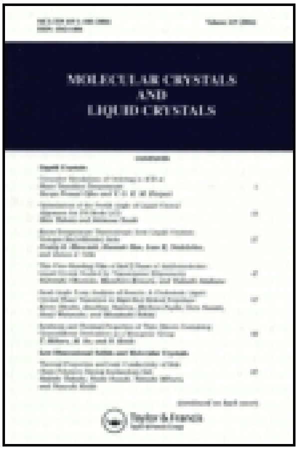

Molecular Crystals and Liquid Crystals Science and Technology. Section A. Molecular Crystals and Liquid Crystals

Publication details, including instructions for authors and subscription information:
http://www.tandfonline.com/loi/gmcl19

Long Period Structure of Langmuir-Blodgeit Multilayer Assemblies

Steven P. Walsh [a] & Jerome B. Lando [a]

[a] Macromolecular Science Department, Case Western Reserve University, Cleveland, OH, 44106

To cite this article: Steven P. Walsh & Jerome B. Lando (1994): Long Period Structure of Langmuir-Blodgeit Multilayer Assemblies, Molecular Crystals and Liquid Crystals Science and Technology. Section A. Molecular Crystals and Liquid Crystals, 240:1, 201-216

To link to this article: http://dx.doi.org/10.1080/10587259408029731

Mol. Cryst. Liq. Cryst. 1994, Vol. 240, pp. 201–216
Reprints available directly from the publisher
Photocopying permitted by license only

Printed in the United States of America

LONG PERIOD STRUCTURE OF LANGMUIR-BLODGETT MULTILAYER ASSEMBLIES

STEVEN P. WALSH, JEROME B. LANDO
Macromolecular Science Department, Case Western Reserve University,
Cleveland, OH 44106

Abstract The structures of cadmium eicosanoate (CdC220AC) and cadmium pentacosa-10,12-diynoate (Cd12-8AC) Langmuir-Blodgett multilayers were studied using x-ray structure analysis methods. The trial and error model refinements indicated the fully ionized salts exist in a linear arrangement where the polar heads of the opposing monolayers are ionically bound with the cadmium ion nested between the carboxylates. The molecular orientation of CdC20AC was found to be normal to the substrate, whereas Cd12-8AC was inclined by about 30° to accommodate the diacetylene moiety. A mechanism for the salt formation upon deposition was rationalized by considering the dissolved counter ions to be loosely bound within the electric double layers of the floating and submerged/deposited monolayers.

INTRODUCTION

Powder diffraction methods have long been of significant importance in elucidating the general structure of Langmuir-Blodgett assemblies.(1) Bilayer thicknesses obtained from Bragg reflections were key evidence supporting the now commonly accepted fact that the molecules in a transferred monolayer preserved the more or less vertical orientation of the condensed floating monolayer, and thus the assembly thickness could be "built-up" systematically by repeated depositions.

Historically, the structural calculations were first applied to determine the general orientation of cadmium eicosanoate molecules. Using a simple step model the researchers noted the observed scattering intensity was predominately dictated by the positioning of the electron rich (cadmium carboxylate) and electron poor (methyl-methyl) regions within the unit cell.(2) More recently, additionally sophisticated models have been proposed by increasing the number of adjustable parameters such as involving the influence of the substrate,(3) or the mosaic nature of the polycrystalline film,(4) or by allowing the position of more atomic centers to independently vary.(5) Due to the limited nature of the data set in this work (typically about 10 observed reflections) specific attempts were made to simplify the approach, and to limit the number of independent variables.

Methods

The structural calculations were performed using the kinematic development of the structure factor (F_{hkl}) using the generalized equation (6) below limited to the $00l$ reflections:

$$|F_{00l}|^2 = \Sigma\, (f_i\cos 2\pi\, l\; z_i)^2 + (f_i \sin 2\pi l\; z_i)^2 \qquad (1)$$

where f_i is the atomic scattering factor of the l center, is the order of the reflection, and z_i is the projection of the ith center onto the l unit cell edge (in fractional distance). For centrosymmetric models the sine terms in the structure factor equation can be neglected since cancellation will cause the terms to sum to zero. The atomic scattering factors for each center at each angle theta wedre calculated from the analytical expression:(7)

$$f\left(\frac{\sin\theta}{\lambda}\right) = \sum_{1}^{4} \left[a_i \exp\left(-b_i\lambda^{-2}\sin\theta\right)\right] + C \qquad (2)$$

where a_i, b_i and c are the appropriate coefficients, and θ is the scattering angle. When applicable the ionized form of the atomic center was selected as the scattering center.

The observed structure factor was obtained from the observed scattering intensity using the relation:

$$I_{00l} = |F_{00l}|^2 Lp \qquad 3)$$

where L and p are the Lorentz and polarization corrections respectively. The polarization factor had the usual form:

$$p = (1 + \cos^2 2\theta)/2 \qquad (4)$$

and the Lorentz factor was that specific to the diffraction geometry:(8)

$$L = 1/\sin^2\theta \cos\theta \qquad (5)$$

where θ is the scattering angle.

The temperature or Debye-Waller factor was considered invariant with respect to θ over the range investigated (1 to 15° 2θ), and thus lumped into the scaling factor. The lumped scale or multiplicity factor, k, was obtained by determining the constant by which, for a specific set of structural model parameters, the reliability index, R, was minimized. An unweighted R factor was calculated by:

$$R = \Sigma\, \frac{|F_c| - k|F_o|}{\Sigma |F_o|} \qquad (6)$$

where F_c and F_o are the calculated and observed structure factors respectively.

To expedite the calculations a modular computer program was written using Microsoft Basic 3.1. The program consisted of six modules for the separate calculation of: the atomic scattering factor, corrected observed structure factor, the fractional coordinates of each atomic center based on the specific model, the calculated structure factor, the scale and reliability index, and data output. Uncorrected observed scattering intensities and model coding could be input for each specific sample data set. The final data were then presented in a 2-d topographic map to facilitate the determination of parameters yielding a good fit.

X-ray scattering data were obtained from Langmuir-Blodgett assemblies of eicosanoic acid (C20AC) and pentacosa-10,12-diynoic acid (12-BAC) deposited on glass from a 10^{-3} M $CdCl_2$ subphase at a pH of 7.0. The transfer pressure was maintained at 30 dynes/cm with a transfer rate of 10 cm/min. Similar samples were deposited on germanium plates as well as aluminum mirrors, and showed the total formation of cadmium carboxylate by transmission and reflection IR spectroscopy.

Samples were mounted in the goniometer of a $\theta/2\theta$ scanning diffractometer with nickel filtered CuKα radiation source (λ=1.5418 Å). The plane of incident x-rays was oriented perpendicular to the deposition direction, reflecting off the deposition surface that faced the moving compression barrier. Diffractograms were obtained from no less than three separate multilayer assemblies of 5.5 bilayers. The bilayer spacing or d_{001} was then obtained by averaging over all observed reflections for all diffractograms. Intensity data from each individual diffractogram were then fit separately and compared. Averaging was not performed since global trends were of interest, and no significant variations were seen between individual data sets.

Maxima of the Bragg reflections and the integrated peak intensities were obtained by fitting ideal Gaussian curves to the observed data using an iterative curve fitting program. Typically, the intensities of the first two observed reflections were neglected in the model calculations due to the limitations of the diffraction geometry at the very low scattering angles, and the appearance of strong subsidiary (Fresnel) maxima.

CdC20AC - Structural Models:

The x-ray diffraction intensity data from samples of cadmium eicosanoate (CdC20AC) were then fit to one of two basic models. The models were similar in their overall construction, but differed in the arrangements of the cadmium ions and carboxylates by allowing for intra- or inter-bilayer complexation of the cadmium. For the intra-monolayer scenario the 2+ charge of one cadmium was countered by two adjacent carboxylates in the same monolayer, resulting, in the head-head region, of two abutting planes of cadmium ions. The inter-monolayer case allowed a more linear salt formation by having the cadmium ion complexed between the carboxylates of adjacent monolayers in a Y-type arrangement.

For both models a fully extended chain was assumed for the aliphatic tail, with the methyl and methylenic hydrogens occupying the same position as their parent carbons. The carboxylate head group was modeled as a carbonyl oxygen located at the alpha-carbon site with the ionic oxygen an incremental step from the alpha-carbon. In the intra-monolayer scenario the distance between the abutting cadmium planes (Cd-Cd) and the cadmium to carboxylate (Cd-O) were allowed to vary from 0.0-3.8Å and 0.0-1.8 Å respectively. The methyl-methyl spacing was fixed, and the incremental step between each atomic center along the bilayer was then determined from the remaining portion of the unit cell divided by the required number of steps (see Figure 1). Upper and lower values for the methyl-methyl distances were considered based on the range of customary values for aliphatic crystals. The values used in the model calculations were 2.6Å and 3.0Å.

The inter-monolayer model was simpler in its arrangement, and was prepared such that half of each cadmium ion occupied the fractional coordinates of 0 and 1. The Cd-0 distance and the methyl-methyl distance were allowed to vary between 0.0-2.0Å and 2.2-4.0Å respectively. Again the incremental step along each atomic center in the bilayer was calculated based on the remaining unit cell fraction (see Figure 2).

CdC20AC - Results and Discussion

From the diffraction data d-spaces were calculated from the observed 00*l* Bragg reflections, and yielded a long period for the CdC20AC bilayer of 55.2 +/_0.3Å. That value was then used as the principal unit cell constraint for the models investigated.

Starting with the CdC20AC case where the cadmium ion was bound in the intra-monolayer fashion, two common features in the results can be observed for both methyl-methyl spaces considered (see Figures 3 and 4). The first is a localized minima region (region of good fit) where the two halves of the cadmium ions are positioned nearly atop one another with the Cd-0 distance being about 1.0Å. The second feature is the tear-drop shape of the minima with the tail extending along a comon diagonal or rift.

In this simple step model, the appearance of a diagonal rift indicates a set of model parameters that results in a common inter-atomic step along the molecular axis. The dotted lines in Figures 3 and 4 correspond to those Cd-Cd and Cd-O distances that produce an average inter-atomic step of 1.27Å. Since a fully extended chain conformation is considered, the average inter-atomic step can be approximated as 1.27 cosϕ,where 1.27 is half of the accepted aliphatic ethylene repeat of 2.54 Å,(9) and ϕ is the average off normal tilt of the molecules. The positioning of the rifts, nearly coincidental with these lines, is a good indication that the molecules are oriented nearly perpendicular to the substrate surface as has been suggested by other x-ray(10) and spectroscopic(11) analyses. The rifting also demonstrates that although the overall appearance of the diffraction data (i.e. the odd-even intensity effect) is predominately due to the regular alternation of high and low electron

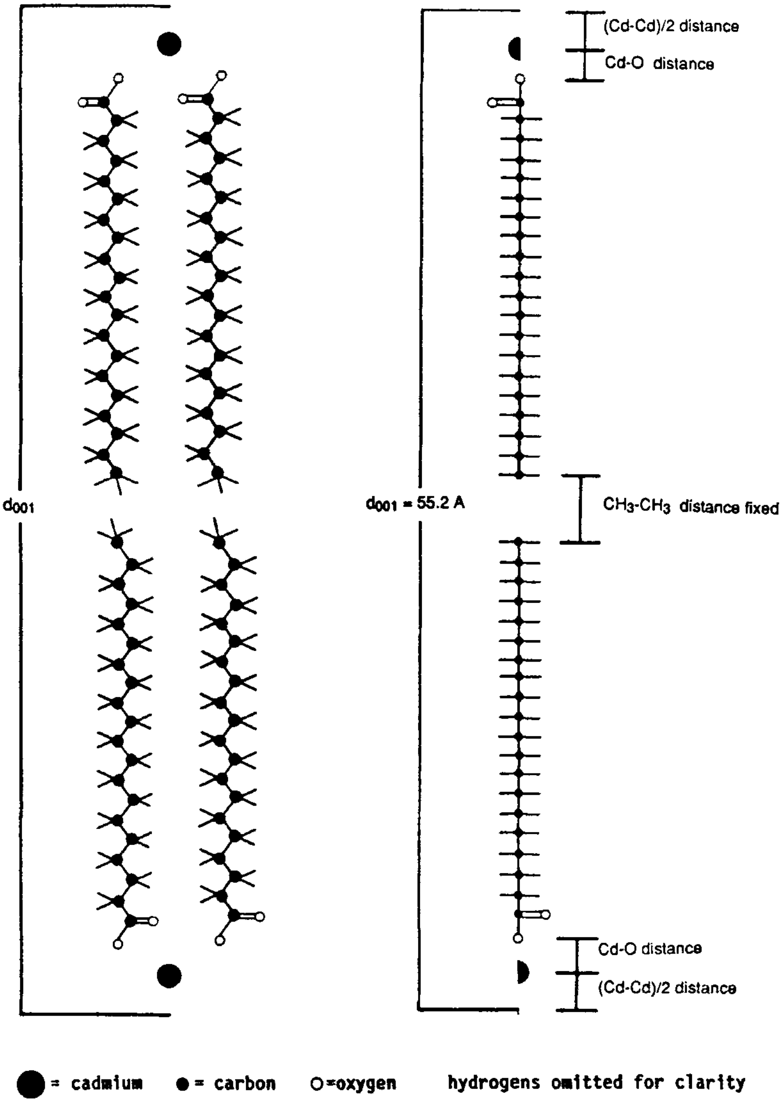

FIGURE 1. An idealized bilayer of cadmium elecosanoate deposited with the counter ion in the intra-monolayer scenario (left), and the corresponding projection step model (right) used in obtaining the calculated structure factor. Cd-Cd and Cd-O distances are allowed to vary as the methyl-methyl distances are fixed. (Note: only C-H bonds are shown for purposes of clarity).

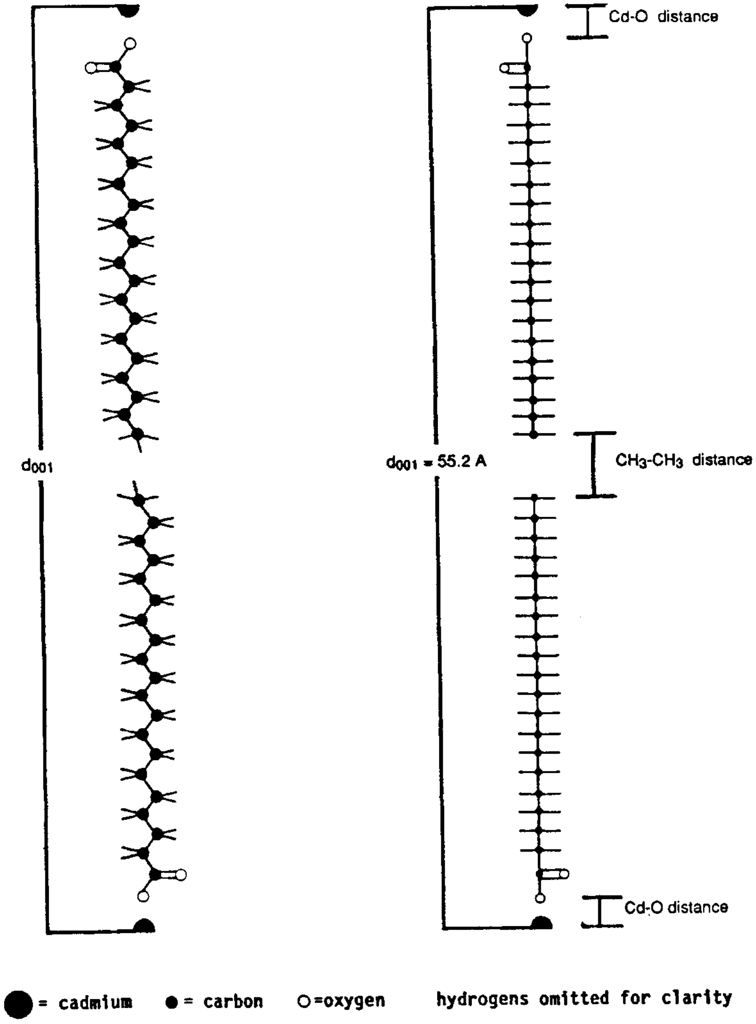

FIGURE 2. An idealized bilayer of cadmium eicosanoate deposited with the counter ion in the inter-monolayer scenario (left), and the corresponding projection step model (right) used in obtaining the calculated structure factor. Cd-O and methyl-methyl distances are allowed to vary. (Note: only C-H bonds are shown for purposes of clarity).

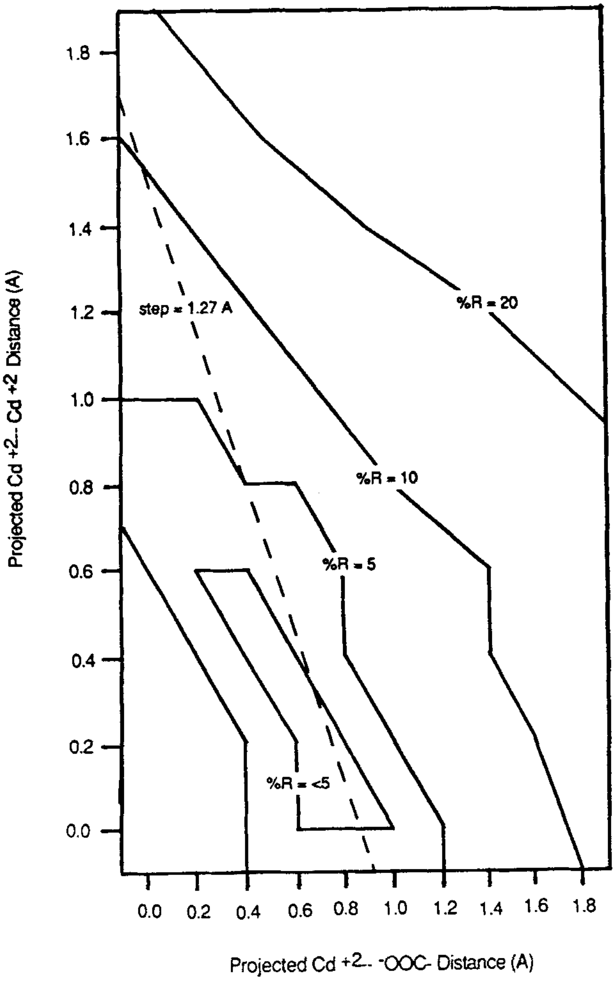

FIGURE 3. Topographic presentation of the calculated residuals for the intra-monolayer case of cadmium eicosanoate where the methyl-methyl distance is fixed to 2.6Å. The broken line indicates model parameters yielding an average inter-atomic step of 1.27Å

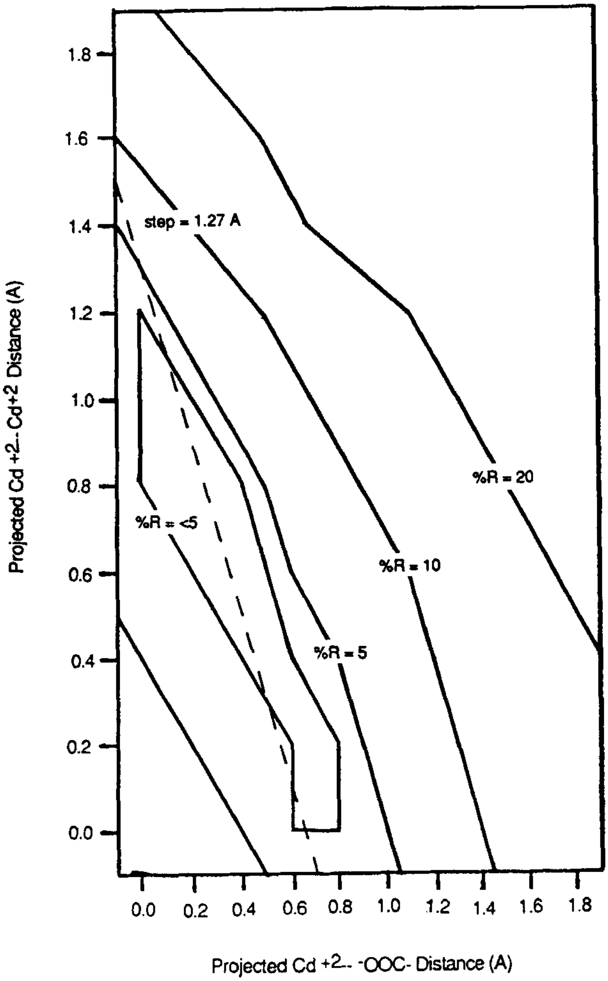

FIGURE 4. Topographic presentation of the calculated residuals for the intra-monolayer case of cadmium eicosanoate where the methyl-methyl distance is fixed to 3.0Å. The broken line indicates model parameters yielding an average inter-atomic step of 1.27Å.

densities through the thickness of the multilayer structure, the intensity is also due to the superposition of the aliphatic tails.

The power of the positioning of the high and low electron density regions can be seen by increasing or decreasing the breadth of the electron free methyl-methyl distance. Increasing the distance to 3.4 Å totally smears the resolution of a structure as the Cd-Cd distance is spread to maintain the effective ratio between the densities in the electron rich and electron poor regions. Similarly, decreasing the methyl-methyl spacing collapses the whole head-head region as the Cd-Cd and Cd-O distances converge to zero.

The significance of the Cd-Cd separation distance lies in the consideration that at a value of zero the intra-monolayer case degenerates into the simpler inter-monolayer case. The observation that both the 2.6Å and 3.0Å methyl-methyl scenarios of the intra-monolayer model yielded Cd-Cd separation values of less than 1.0Å, or the sum of the Cd^{+2} radii, strongly suggests that salt formation occurs between two monolayers upon deposition, or that rearrangement subsequently takes place. The linear inter-monolayer model is more in keeping with the accepted structures of divalent cation/fatty acid salts,(12) nonetheless structures of the intra-monolayer case have been routinely reported in the literature.

Figure 5 shows the results for the inter-monolayer model as the Cd-O and methyl-methyl distances are varied between 0.0-2.0 and 2.2-4.0Å respectively. In accordance with the degenerated intra-monolayer cases, the region of best fit for the inter-monolayer model occurs at a Cd-O distance of about 0.8Å and a methyl-methyl separation of 2.8Å. The combination of these parameters again produces an inter-atomic step of 1.27Å along the multilayer assembly, or a projection of the planar zig-zag repeat of 2.54Å, indicating a vertical orientation.

Cd12-8AC - Structural Model

Based on the results for CdC20AC an analogous simple step model with the cadmium ion complexed in an inter-monolayer fashion was considered for the assemblies of cadmium pentacosa-10,12-diynoate (Cd12-8AC, see Figure 6). The structure of the carboxylate was again modeled with the carbonyl oxygen located at the alpha-carbon, and the ionized oxygen an incremental step away. The hydrophobic tail was represented as a simplified aliphatic chain with the exclusion of methylenic hydrogens at the appropriate diacetylenic carbons. As such the kink in the tail caused by the six co-linear carbons of the diacetylene was neglected. The model was refined by allowing the Cd-O and methyl-methyl separation distances to vary between 0.1 - 1.9 Å and 0.2 - 4.0 Å respectively.

Cd12-8AC - Results and Discussion

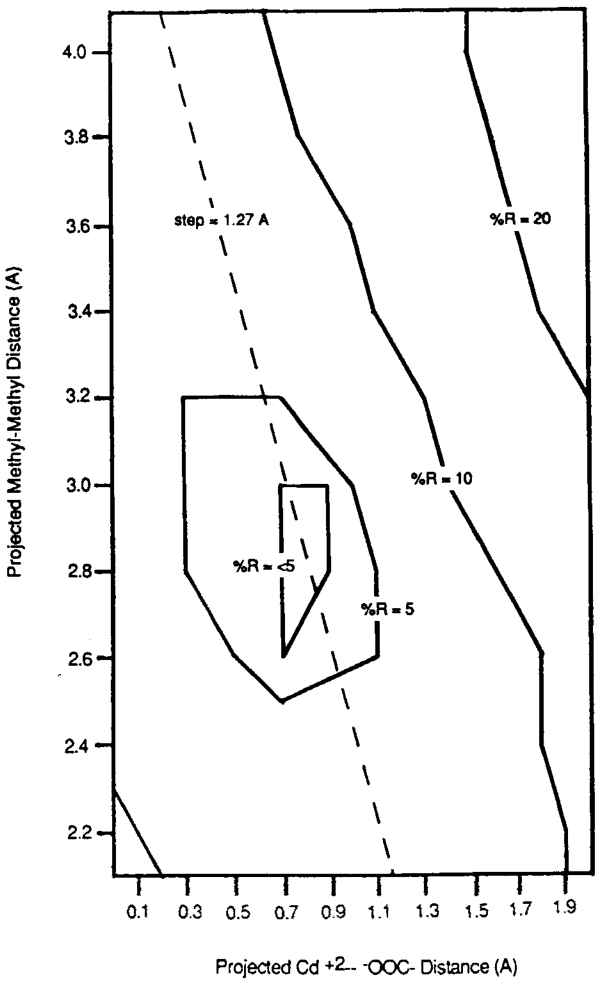

FIGURE 5. Topographic presentation of the calculated residuals for the inter-monolayer case of cadmium eicosanoate. The broken line indicates model parameters yielding an average inter-atomic step of 1.27Å.

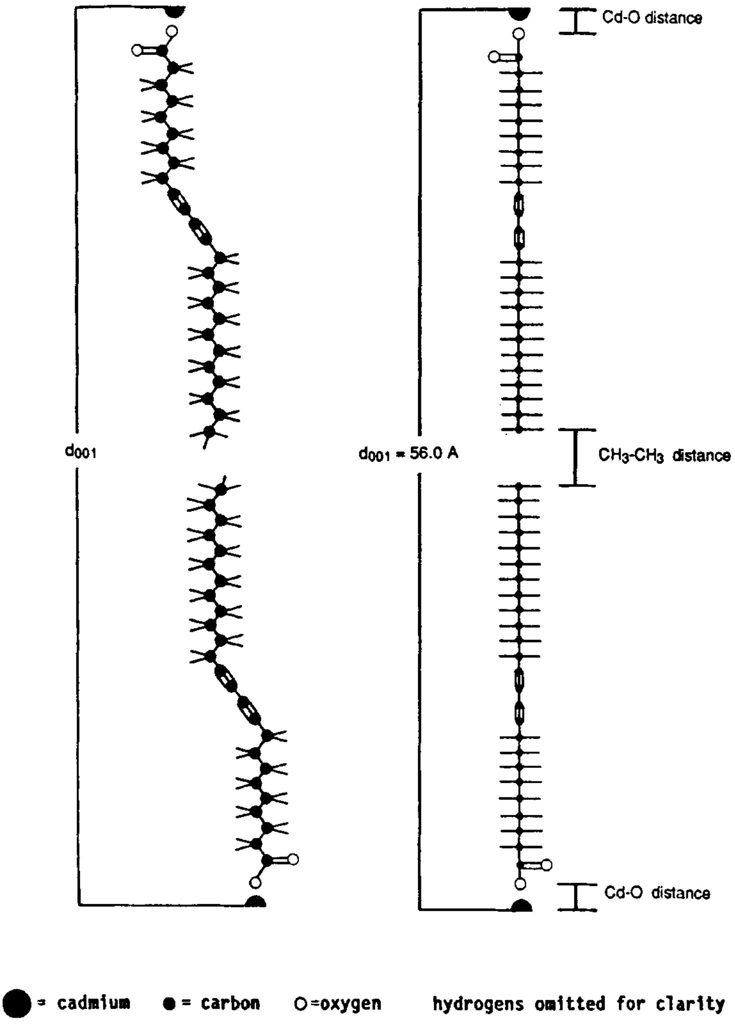

FIGURE 6. An idealized bilayer of cadmium pentacosa-10,12-diynoate with the counter ion in the inter-monolayer scenario (left), and the corresponding projection step model (right) used in obtaining the calculated structure factor. Cd-O and methyl-methyl distances are allowed to vary. (Note: only C-H bonds are shown for purposes of clarity).

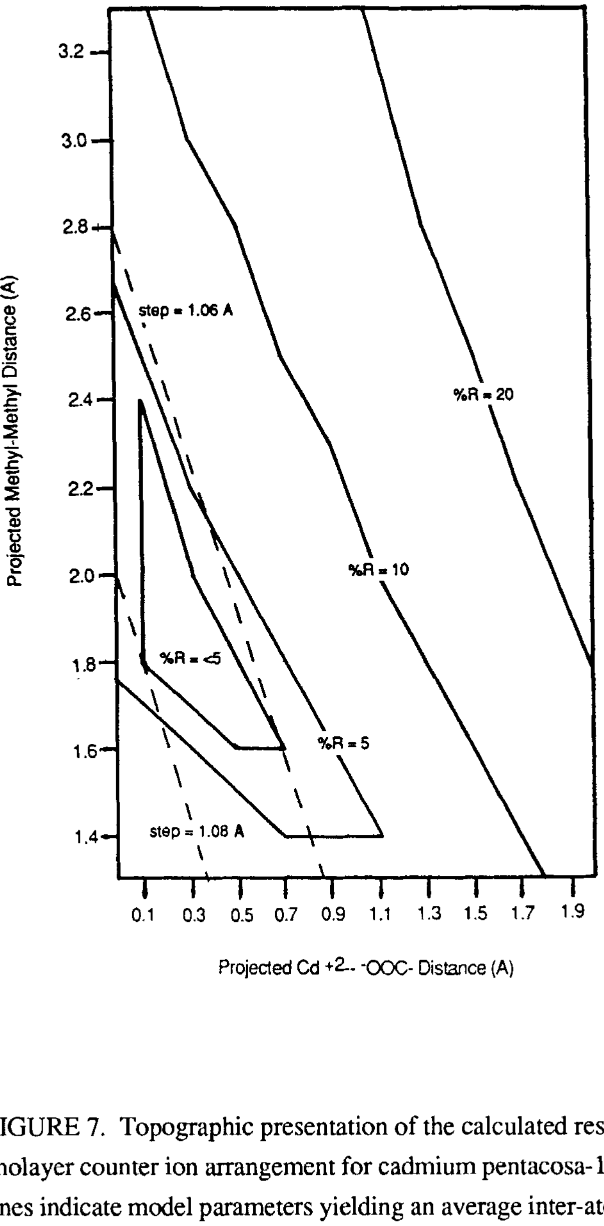

FIGURE 7. Topographic presentation of the calculated residuals for the purposed inter-monolayer counter ion arrangement for cadmium pentacosa-10,12-diynoate. The broken lines indicate model parameters yielding an average inter-atomic step of either 1.06Å or 1.08Å. The axial tilt can be approximated as $\phi = \cos^{-1}$ (step/1.27).

The Bragg maxima in the case of Cd12-8AC yielded an average bilayer long period of 56.0 +/- 0.5Å. For comparison with the previous models the results shown in Figure 7 have been truncated to show only the relevant section of the data. As has been previously noted, an obvious rifting in the data presentation can be seen, with an apparent Cd-O and methyl-methyl minima at about 0.2Å and 2.0Å respectively.

Unlike the structures of CdC20AC, the rifting in the diacetylenic compounds shows an average inter-atomic step of 1.07Å, or an off axis tilt of about 33°. This molecular orientation is in good agreement with the structures proposed by Lieser, Tieke, and Wegner(13) for Cd12-8AC by electron diffraction, as well as the homolog lithium nonacosa-10,12-diynoate (Li16-BAC) seen by Day and Lando,(14) which both showed an axial tilt of about 30°. The degree of tilt is reasonable when considering the packing requirements of the diacetylene groups.

The positioning of the cadmium ion relative to the carboxylate anion found is also in good agreement with the cation positioning of other soaps demonstrating a high degree of axial tilt. Single crystal structural analysis of potassium caproate(15) showed the cation to be nested within the carboxylate presenting a projected separation of only 0.3Å, with the carbonyl oxygen projection being very close to the alpha-carbon. In the case of a divalent cation the same is possible by allowing the cation to be nested between the two opposing carboxylates in adjacent monolayers.

Although the methyl-methyl projection seems prohibitively small, the value can be justified by compensating for the tilt which results in a linear separation of about 2.7Å. Electron diffraction studies of diacetylenic multilayer assemblies (13) have shown well defined reflections for an orthogonal electron beam indicating a high degree of registry between subsequent monolayers. Thus if registry of the aliphatic portions in the structures exists, then our observation is quite reasonable.

Deposition of Ionized Monolayers

The mechanism of the salt formation that allows for the observed structure can be rationalized by considering the ionic occurrences at the polar interfaces of the floating and deposited monolayers. In the most general case, fully ionized floating monolayers, the counter ions are not bound to the individual molecules in the monolayer, but exist in the electric double layer as described by an ideal Gouy-Chapman model.(16) The thickness of the double layer, and thus the mobility of the ions, is determined by a number of conditions such as pH, ionic concentration, and the chemistries of the charged species (both the dissolved ions as well as the monolayer molecules).

Upon, for convenience, the deposition down-stroke the floating monolayer is transferred to the substrate, pulling the required counter ions (still freely mobile within the transferred double layer) with it. On the subsequent deposition up-stroke the double layers of the floating and deposited monolayers overlap and interact at the three phase contact line (see Figure 8). Due to the mobility of the counter ions, the increasing ionic concentration at the juncture forces ionic migration to occur, and as the subphase drains the salt is formed. Sufficient mobility is afforded in this process to allow a linear salt to be formed. The two monolayers are thus ionically bound together, and the entrained water is forcibly exuded resulting in a dry or "reactive"(17) deposition. The forcible exudation of the water by divalent cations, as well as the resulting dry deposition, has long been observed (18) and exploited in an effort to rapidly produce multilayered assemblies from fatty acids and acid analogs.

CONCLUSIONS

By matching calculated and observed diffraction intensities for idealized multilayers of CdC20AC and Cd12-8AC generalized structures were elucidated. Salt formation by the divalent cations seems to occur in a linear fashion between two separate monolayers. For multilayers of CdC20AC the axes of the molecules in the assembly are seen to be oriented nearly perpendicular to the surface as demonstrated by an average aliphatic projection repeat of 2.54Å. In order to accommodate the diacetylenic kink, multilayers of Cd12-8AC are inclined by about 30^o as seen by the average aliphatic projection of 1.07Å.

A deposition mechanism allowing the proposed ionic structure can be rationalized by considering appreciable ionic mobility of the dissolved counter ions during the deposition process. The overlap of the electric double layers and resulting excess concentration of cations at the deposition line suggested by this mechanism helps to explain the observation of more efficient depositions upon the addition of trace quantities of divalent cations. Charge neutrality is preserved as the salt is formed with the cation nested between two carboxylates in adjacent monolayers. Such an arrangement is in agreement with the structures observed for bulk crystals of other divalent cation/fatty acid salts.

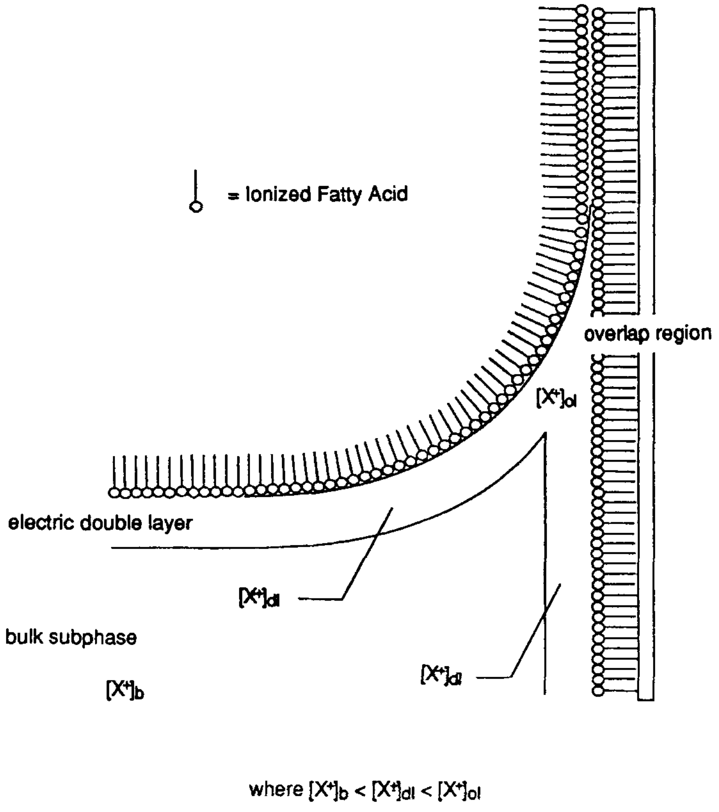

FIGURE 8. Schematicized representation of the deposition process for ionized floating monolayers. Ionic mobility and an increasing concentration gradient between the bulk subphase (b), the simple double layer region (dl) and the region of double layer overlap (ol) at the three phase contact line drives the reactive process yielding a linear salt between the two deposited monolayers. Ionic binding of the polar heads is thus responsible for exuding the entrained subphase resulting in a dry deposition.

REFERENCES

1. G.L. Clark, R.R. Sterrett, and P.W. Leppla, J. Am. Chem. Soc., 1935, 57, 330.
2. A. Matsuda, M. Sugi, T. Fukui, S. Iizima, M. Miyahora, and Y. Otsubo, J. Appl. Phys., 1977, 48, 771.
3. K. Mizushima, T. Nakayama, and M. Azuma, J. Appl. Phys., (Japan), 1987, 26, 772.
4. K. Mizushima, S. Egusa, and M. Azuma, J. Appl. Phys., (Japan), 1988, 27, 715.
5. P. Fromhertz, U. Oeschlagel, and W. Wilke, Thin Solid Films, 1988, 159, 421.
6. L.V. Azaroff in, Elements of X-Ray Crystallography, McGraw Hill: New York, 1968, Chapters 10 and 11.
7. International Tables for X-Ray Crystallography, Volume 4: Knoch Press; Birmingham, England, 1974, pp. 71-101.
8. M. Buerger in Crystal Structure Analysis: Wiley Interscience: New York, 1960, pp. 171-174.
9. B.K. Vainstein and Z.G. Pinkster, Dokl. Akad. Nauk. USSR, 1950, 72, 53.
10. T. Fukui, M. Sugi, and S. Iizima, Phys. Rev. B, 1980, 22, 4898.
11. J. Umemura, T. Kamata, T. Kawai, and T. Tanenaka, J. Phys. Chem., 1990, 94, 62.
12. J.F. Stephens and C. Tuck-Lee, J. Appl. Cryst., 1969, 2, 1.
13. G. Lieser, B. Tieke, and G. Wegner, Thin Solid Films, 1980, 68, 77.
14. D. Day and J.B. Lando, Macromolecules, 1980, 13, 1483.
15. V. Vand, T.R. Lomer, and A. Lang, Acta Cryst., 1949, 2, 214.
16. E.J.W. Verwey and J.T.G. Overbeek in Theory of the Stability of Lyophobic Colloids; Elsevier, Amsterdam, 1948.
17. G.L. Gaines, Jr., in Insoluble Monolayers at Liquid-Gas Interfaces: Interscience: New York, 1966, pp. 326-333.
18. K.B. Blodgett and I. Langmuir, Phys. Rev., 1937, 51, 964.